JOURNAL OF APPLIED POLYMER SCIENCE VOL. 21, 2375–2392 (1977)

Use of Auger and X-Ray Photoelectron Spectroscopy to Study the Locus of Failure of Structural Adhesive Joints

M. GETTINGS, *Materials Development Division, AERE Harwell, Oxfordshire, England,* and F. S. BAKER and A. J. KINLOCH, *Ministry of Defence, ERDE, Waltham Abbey, Essex, England*

Synopsis

The techniques of Auger electron spectroscopy (AES) and x-ray photoelectron spectroscopy (XPS) have been used to study the locus of failure of epoxy resin joints. The effects of a long water immersion and the application of a silane-based primer have also been studied. Results indicated that for dry joints fracture occurred near an epoxy resin/metal interface while with water-soaked unprimed joints, fracture occurred interfacially between the adhesive and iron oxide. The application of the primer to the metal surface prior to bonding prevented the formation of a water-formed oxide although fracture was then found to occur through the primer.

INTRODUCTION

Epoxide resin-based structural adhesives cure to form thermosetting rigid polymers and are extensively used for joining metals, plastics, carbon- and glass-reinforced composites, etc., in many diverse industries. However, a serious limitation frequently encountered in the use of structural adhesives is the deleterious effect which moisture has upon the strength of a bonded component, especially when the component is also subjected to conditions of relatively high stress and temperature.[1,2] Unfortunately, the fundamental mechanisms leading to this loss of strength have not, as yet, been completely elucidated; correlations between accelerated and outdoor weathering tests are poor, and predictions of the stability of joints exposed to hostile environments are correspondingly unreliable. Consequently, the logical selection of materials and techniques to avoid joint failure has been severely restricted.

A major consideration in identifying the mechanics and kinetics of adhesive joint failure is the locus of fracture, i.e., whether the joint failed by cohesive fracture of the adhesive or the substrate, interfacially between the adhesive–substrate interface (it has been argued that true interfacial failure can never occur[3]), or a complex mixture of these possible failure paths. The poor durability of adhesive joints has been ascribed to (a) stress hydrolysis of covalent bonds in a boundary layer of adhesive close to the interface,[4] (b) hydration of the oxide surface, invariably present on most metallic substrates, which then is mechanically weak and causes premature joint failure,[5] or (c) the displacement of the

adhesive on the substrate surface by water resulting in interfacial failure.[6,7]

In spite of the lack of fundamental knowledge concerning the mechanisms of environmental failure, it has been established empirically that the use of silane-based primers at the adhesive–substrate interface may lead to considerable increases in joint durability. It is sufficient to note here that the most common type of silane primers employed have the general structure $X_3Si(CH_2)_nY$, where $n = 0$ to 3, X is a hydrolyzable group on silicon, and Y is an organofunctional group selected for compatibility with a given adhesive. The generally, but not universally, accepted mechanism by which the durability of the joint is increased is the formation of strong, covalent interfacial bonds. For the substrate–silane interface, this arises from the formation of ≡Si—0—substrate bonds; and for the adhesive–silane interface, from the reaction of the Y group on the silane with reactive groups in the adhesive. However, other features, such as wetting[8] and the possible formation of a boundary layer in the adhesive, differing in chemical and physical properties to that of the bulk resin, must be considered.[9] Experimentally, silane primer films have been found[10] to be polymeric, composed of a strongly held polysiloxane network along with some hydrolyzed or partially hydrolyzed silane and small polysiloxane molecules.

The aim of the present study is to use Auger electron spectroscopy (AES)[11,12] and x-ray photoelectron spectroscopy (XPS)[13] to identify the modes of failure for joints consisting of mild steel substrates bonded with an epoxide adhesive. The effects of water immersion and the use of a silane-based primer on the joints will be described.

AES and XPS are particularly suited for examining fractured adhesive joints as both are surface techniques sampling to a depth not With XPS, chemical information can be derived by studying the shift in binding energy of an atom bound near the surface from that expected for a neutral atom. The far more complex nature of the Auger process does not, in general, lend itself so easily to such interpretation.

The two techniques are, in many ways, complementary. In Auger electron spectroscopy, Auger electrons are excited from surface atoms with a small-diameter electron beam (1–50 μ), thereby giving good spatial resolution. In this work, a 30–μm diameter beam is used, but useful spectra have been obtained with probes 0.3 μm in diameter.[13] Since XPS depends on x-ray photons to excite photoelectrons, spatial resolution comparable to AES cannot as yet be obtained. The advantage of XPS is, however, that charging effects are minimized and surfaces of insulators can be analyzed. In the work described, both conducting (using AES and XPS) and insulating surfaces (using XPS) were examined.

EXPERIMENTAL

The Analysis System

The AES/XPS techniques are housed in a vacuum chamber capable of being pumped to 3×10^{-11} torr using a combination of turbomolecular and sublimation pumps. In the experiments reported here, pressures were in the region of 5×10^{-10} torr before and after fracture. On fracture, released gases could be monitored with a residual gas analyzer.

Auger electrons and photoelectrons emitted from a solid surface are detected

using a double-pass cylindrical mirror analyzer (CMA) supplied by Physical Electronics Inc. (PHI) and whose principles of operation have been described by Palmberg.[14] In the AES mode, Auger electrons are generated from a 30μm diameter spot during bombardment by electrons from a coaxial 0–5-keV electron gun. During transmission through the analyzer, electrons pass through 1-mm-diameter apertures which effectively define the resolution measured as 0.7% at 2 keV and enter a channel electron multiplier for amplification. Operating conditions are conventional in that the swept potential on the outer cylinder is modulated and the multiplier signal detected using a lock-in amplifier.

In the XPS mode, two spherical retarding grids between the specimen and the first aperture are used as electron velocity filters; in the AES mode, these grids are grounded. On passing through the grids, photoelectrons are retarded from their initial kinetic energy to a fixed band-pass energy which can be preselected in the range of 5–200 eV. To obtain greater sensitivity, the apertures are changed from 1 mm to 3.75 mm in diameter by means of a rotatable feedthrough. The specimen is flooded with Al K_α x rays of characteristic energy 1486.6 eV, and the photoelectrons ejected are accepted into the analyzer from an approximately circular area of about 7 mm^2. The x-ray source (600 W max) is some 10 cm from the analysis point, and surfaces are irradiated at 60 degrees to the normal.

The mild steel specimens bonded with epoxy resin were mounted (up to five at a time) on a carrousel which was fitted to a manipulator in such a way that each specimen could be maneuvered individually into the jaws of a fracture attachment (PHI Model 10–520). Fracture was achieved inside the vacuum system by striking the side of the sample with a small hammer, following which the section attached to the carrousel was moved until the fracture surface was in the optimum position for analysis.

Since the same analyzer is used for both AES and XPS, and optimum specimen positions for the two techniques are coincident. At this position, the surface under analysis can be eroded by sputtering with a 2-keV Ar ion gun (PHI Model 04-167) having a maximum current density of 80 μA/cm^2; in this study, the gun was used to profile through epoxy or oxide films on the fractured surfaces.

After AES and XPS analyses, the fractured joints were transferred to a scanning electron microscope and both low- and high-magnification photographs were obtained from the fractured surfaces.

Specimen Preparation

Two mild steel (BS 970, EN3B) stubs, 3.7 mm in diameter and of respective lengths 19.5 and 8 mm, were bonded together to form a fracture sample using a standard adhesive and curing agent. The surfaces to be bonded were first immersed in a degreasing bath of trichloroethylene, then grit blasted with 180–220 mesh alumina, then degreased again, and finally air dried. The adhesive used was a diglycidyl ether of bisphenol A (Epikote "828" epoxy resin Shell Chemicals Ltd) mixed with 9.4 wt-% of a curing agent (HY 959 Ciba-Geigy U.K. Ltd).

Of the three series of samples (five specimens per series), two were bonded with only the above-mentioned adhesive, while for the remaining series, the steel was coated with a primer Union Carbide A187 (1% γ-glycidoxylpropyltrimethoxy-

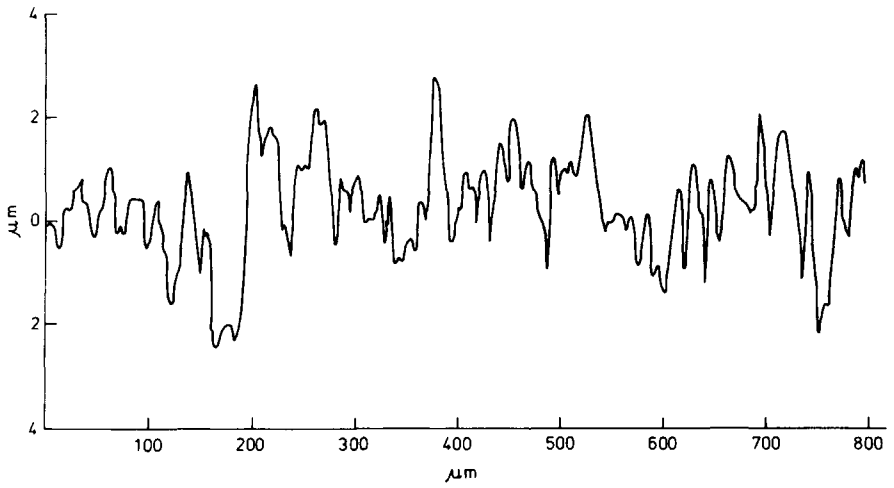

Fig. 1. Typical Talysurf profile of an abraded mild steel surface prior to coating with epoxy resin.

silane aqueous solution) prior to bonding with the 828/959 adhesive/curing agent. All bonds were established by curing at 23°C for 96 hr, followed by 100°C for 1¼ hr, and finally 180°C for 2¼ hr. After the cure the specimens were allowed to cool slowly.

TABLE I
Mild Steel Reference Sample. Variation in Surface Concentration of Elements Detected by XPS[a]

Element	Surface concn., atomic % as received	Surface concn. after indicated amount of material removed		
		50 Å	150 Å	400 Å
Fe	18.8	32.4	60.6	70.7
O	56.3	43.5	27.7	20.8
C	19.7	8.5	4.2	1.8
Al	trace	15.6	7.5	6.7
Mn	2.7	—	—	—
Zn	2.5	—	—	—
Cu	—	—	—	—

[a] Estimated error ± 15%.

TABLE II
Mild Steel Reference Sample. Variation of Binding Energy of Iron, Carbon, and Oxygen Detected at surface[a]

Element	Binding energy eV, as received	Binding energy after indicated amount of material removed		
		50 Å	150 Å	400 Å
Fe	710.2	706.6 710.0 (Sh)	706.0	705.9
O	529.8	530.5	530.2	530.5
C	285.0	284.8	284.5	284.7

[a] Sh = Shoulder on main peak. Error on peak position ± 0.4 eV.

Two of the three series (one unprimed joint and one primed joint) were soaked for one calendar month in distilled water at 60°C prior to analysis to investigate the influence of a water environment on bonding.

RESULTS

The Cleaned Steel Surface

Scanning electron micrographs and Talysurf measurements of the abraded mild steel surface established that the surface was rough, with peak-to-valley readings being several microns. A typical Talysurf profile is shown in Figure 1. The resolution of the instrument is not sufficient, however, to show the deep fissures and microcracks which were almost certainly present.

XPS and AES analyses of the cleaned mild steel surface were performed for the as-cleaned condition and as a function of depth into the surface. The latter was achieved by analyzing the surface after it had been eroded away by argon ion bombardment. The amount of material calculated to have been removed by this process is estimated to be in error by ±20%. The results of the XPS analyses are presented in Tables and I and II. It should be noted that throughout this work, the photoelectron yields from which atom concentrations are obtained have been corrected for the variation in sensitivity of each element to the XPS

TABLE III
Dry Unprimed Joint. "Metal" Surface: Variation in Surface Concentration of Elements Detected by XPS[a]

Element	Surface concn., atomic % freshly fractured surface	Surface concn after indicated amount of material removed	
		50 Å	130 Å
Fe	19.3	47.3	50.2
O	53.2	27.9	25.0
C	26.3	20.0	20.1
N	0.5	—	—
Cl	0.7	—	—
Al	trace	4.8	4.7

[a] Estimated error ± 15%.

TABLE IV
Dry Unprimed Joint. "Metal" Surface: Variation of Binding Energy of Iron, Oxygen, and Carbon

Element	Binding energy, eV freshly fractured surface	Binding energy after indicated amount of material removed	
		50 Å	130 Å
Fe	709.7	706.5	706.7
	706.5 (Sh)[a]	710.0 (Sh)	710.0 (Sh)
O	534.5	530.7	530.6
	530.5 (d)[a]		
C	286.4	284.0	284.3

[a] Sh = Shoulder on main peak; d = doublet. Error ±0.4 eV.

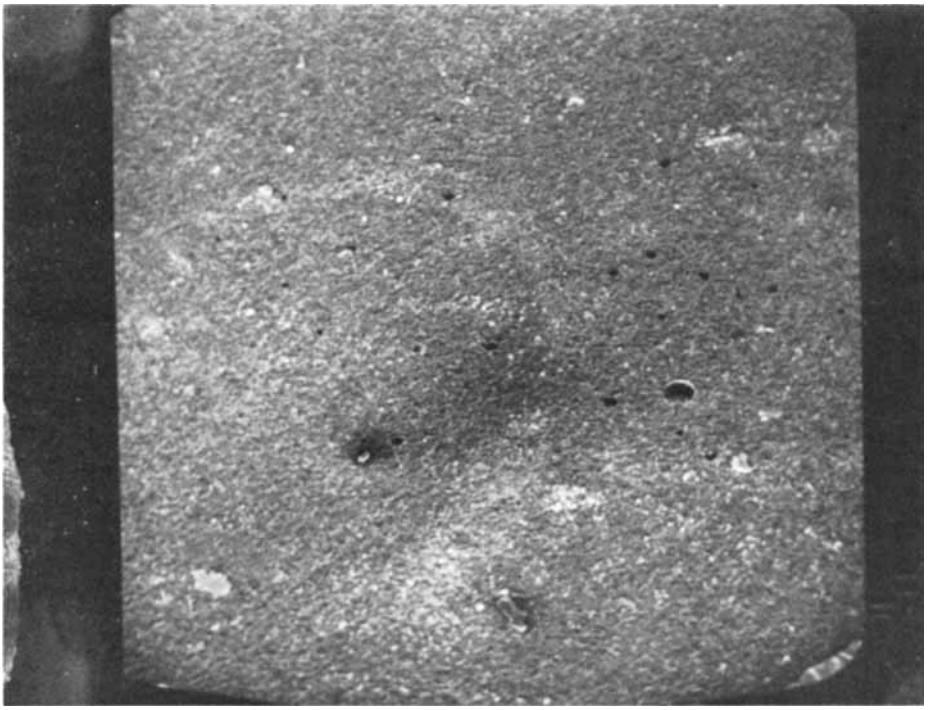

Fig. 2. Auger electron spectroscopy "line scans" of iron, carbon, and oxygen taken across a fracture surface immediately after fracture and at a depth of about 50 Å.

technique. Earlier work[15] on pure elements indicated that variations in reported sensitivities could lead to errors of ±15% in atomic concentration calculations. Binding energies (*BE*) are quoted to an accuracy of ±0.4 eV and are related to the position of the gold $4f_{7/2}$ photoelectron peak.

Comparison of the binding energies quoted by Hirokawa et al.[16] for iron and its oxides with those found on the mild steel specimen shows that the surface was covered with an iron oxide, probably Fe_2O_3. It is also evident that on ion bombardment, the oxide was progressively removed until, at a depth of 150 Å, only pure iron (*BE* 706.0 eV) was detected suggesting that the oxide layer was between 50 Å to 150 Å thick.

The position of the oxygen peak is the same as that found for oxygen in metal oxides,[16–19] and the concentration of the element on the surface can be assigned to the oxides of the metals found. After removal of 400 Å of the surface an appreciable quantity (~20%) of oxygen was still present. Two metals were detected at this depth, aluminum and iron; and since the iron was in the metallic state, only the Al could have been associated with this oxygen. The aluminum must have originated from alumina particles embedded in the metal surface during the grit blasting process. At first inspection, the aluminum–oxygen ratio does not appear correct, but Coad[20] has found that prolonged ion bombardment of alumina reduces the aluminum–oxygen ratio to a value close to that measured here.

The 1*s* carbon photoelectron peak at 285.0 eV can be associated with elemental carbon or hydrocarbon.[21,22] On ion bombardment, the carbon concentration decreased such that, at 400 Å, it constituted only 2% of the total atom concen-

tration. Since the particular steel used in these experiments contained only 0.25% of carbon, the excess carbon probably existed as contamination residing within deep fissures or as carbides formed as a result of the ion bombardment.

In addition to the elements detected by XPS, AES revealed the presence of nitrogen, chlorine, sulfur, and sodium, all common surface contaminants which were easily removed by a light ion bombardment.

Dry Unprimed Joints

On fracture, each joint released a small quantity of gas which raised the system pressure momentarily from 5×10^{-10} torr to 5×10^{-9} torr. To the eye, the fracture appeared purely interfacial, leaving two faces, one of which was covered with adhesive while the other was apparently bare metal. One of the five samples broke in such a way that the surface covered with adhesive (here called the "epoxide" surface) could be analyzed while the other four broke, offering an apparently clean metal surface (here called the "metal" surface) for analysis.

The XPS data from the metal surface listed in Tables III and IV show that the iron detected was in both the metallic (*BE* 706.5 eV) and oxidized (*BE* 709.7 eV) states. The oxygen peak at 530.5 eV can readily be ascribed to oxygen in the iron oxide, while the oxygen species with a binding energy of 534.5 eV may

TABLE V
Dry Unprimed Joint. Epoxide Surface: Variation in Surface Concentration of Elements Detected by XPS[a]

Element	Surface concn., atomic %, freshly fractured surface	Surface concn. after indicated amount of material removed		
		50 Å	130 Å	1150 Å
Fe	6.6	14.5	20.1	11.6
O	33.2	9.7	10.9	13.9
C	42.7	63.7	52.1	70.8
N	5.1	2.4	4.0	—
Cl	12.4	9.7	12.9	3.7
Al	trace	trace	trace	trace

[a] Estimated error ± 15%.

TABLE VI
Dry Unprimed Joint. Epoxide Surface: Variation of Binding Energy of Iron, Oxygen, and Carbon[a]

Element	Binding energy, eV, freshly fractured surface	Binding energy after indicated amount of material removed		
		50 Å	130 Å	1150 Å
Fe	713.4	712.5	710.2 707.5 (Sh)	708.8
O	535.4	533.7	532.2	531.5
C	288.0	286.2		
	289.5 (Sh)	289.2 (Sh)	284.7	284.2

[a] Sh = Shoulder on main peak. Error ± 0.4 eV.

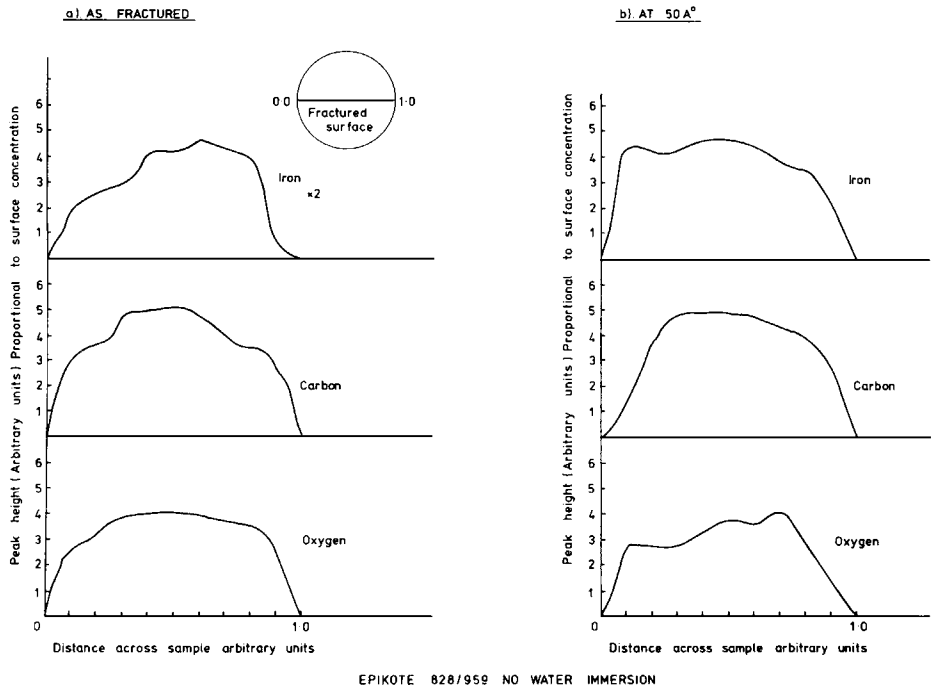

Fig. 3. Scanning electron micrograph (SEM) of an epoxy-covered surface—note the appearance of holes as black spots distributed over the surface. Magnification is ×50.

be associated with the carbon 1*s* peak at 286.4 eV, as both peaks disappear after a small amount of iron bombardment.

Significant changes in the concentrations of the elements occurred when 50 Å of the surface were removed. The amount of iron increased, with the majority of the element existing in the metallic form; the oxygen peak at 534.5 eV disappeared, and the carbon photoelectron peak shifted to 284.0 eV. This carbon peak shift could have been due either to the removal of the higher binding energy species of carbon to reveal the lower binding energy form or the reduction of the original carbonaceous material to carbon by ion bombardment.

Although further erosion of the surface to a depth of 130 Å produced no major changes in the concentrations of the elements detected, a close examination of the iron photoelectron peak shape shows that at this depth, the amount of oxidized iron present decreased from 50% to 30% of the total iron concentration.

AES analyses were performed on the "metal" surface at various points after fracture and ion bombardment. In addition, the variation in concentration of an element across a surface was achieved by monitoring a selected Auger electron peak as the sample was moved through the electron beam. The results from these "line scans" for carbon, oxygen, and iron are summarized in Figure 2 from the as-fractured surface and from a depth of 50 Å. It appears that all elements were evenly distributed across the sample, particularly after 50 Å were removed. The AES results supported the XPS analyses in that ion bombardment caused the iron concentration to increase and the oxygen concentration to decrease.

Study of the epoxide surface of the joint by XPS (Tables V and VI) revealed several interesting effects. Iron, for example, exhibited a peak at a binding energy of 713.4 eV which could not be identified with iron in dry iron oxides. This

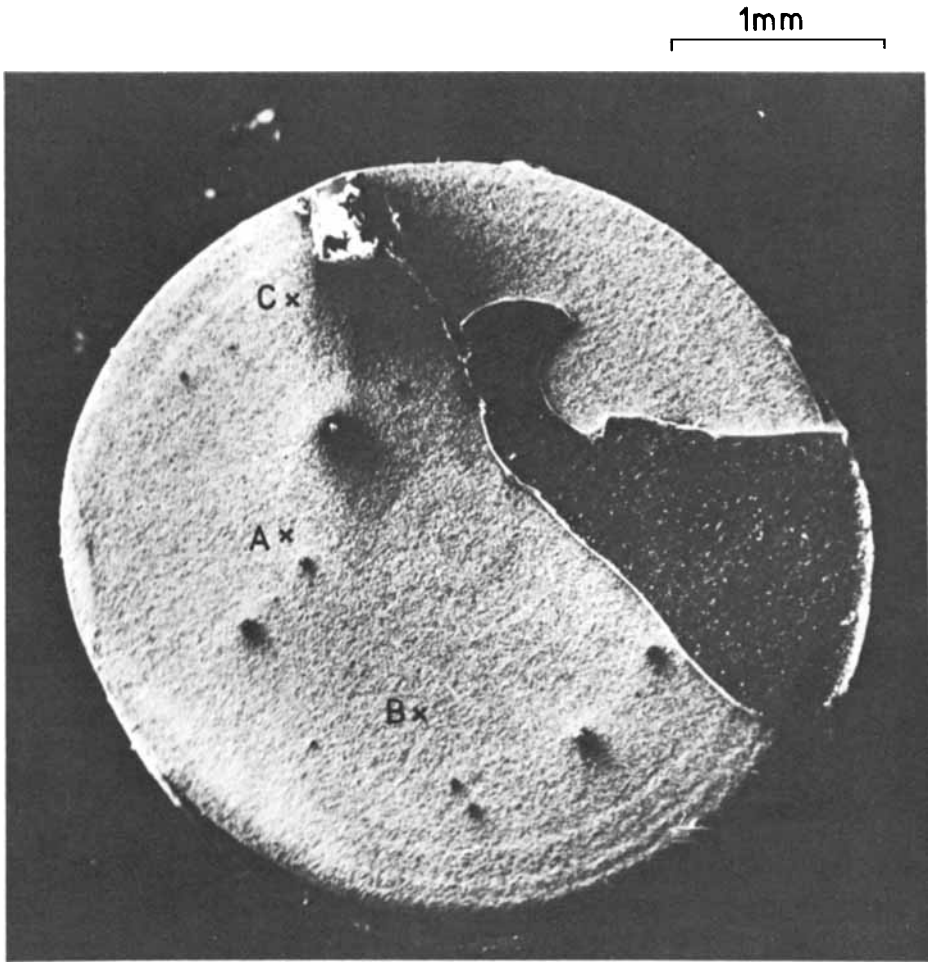

Fig. 4. Typical SEM of a fracture surface showing both metal surface and epoxy resin lump (dark area middle right). AES performed in areas A, B, and C.

high-energy species was also observed on the freshly fractured surfaces of the silane-treated joints, while one with an even higher binding energy was found on the surface of the water-soaked unprimed samples. Associated with these high-energy peaks were oxygen species ranging in binding energy from 536.2 to 535.5 eV. It has been demonstrated[19] that water condensed on aluminum, manganese, and magnesium gives oxygen signals corresponding to binding energies from 535.0 to 535.6 eV, while oxygen in the hydroxides of these metals gives rise to peaks in the range 532.6 to 533.5 eV. It is proposed, therefore, that the high binding-energy species of iron and oxygen observed in this present study are due to heavily hydrated iron oxide to which may be attached chemisorbed water.

A further intriguing feature of the epoxide fractured surface was the detection of a significant quantity (~12%) of heavily oxidized iron at a depth of 1150 Å. There is strong evidence, from scanning electron microscopy studies of the surface (see, for example, Fig. 3), that holes exist in the epoxy resin. This evidence is further supported by earlier work from a mild steel/epoxide/stainless steel joint

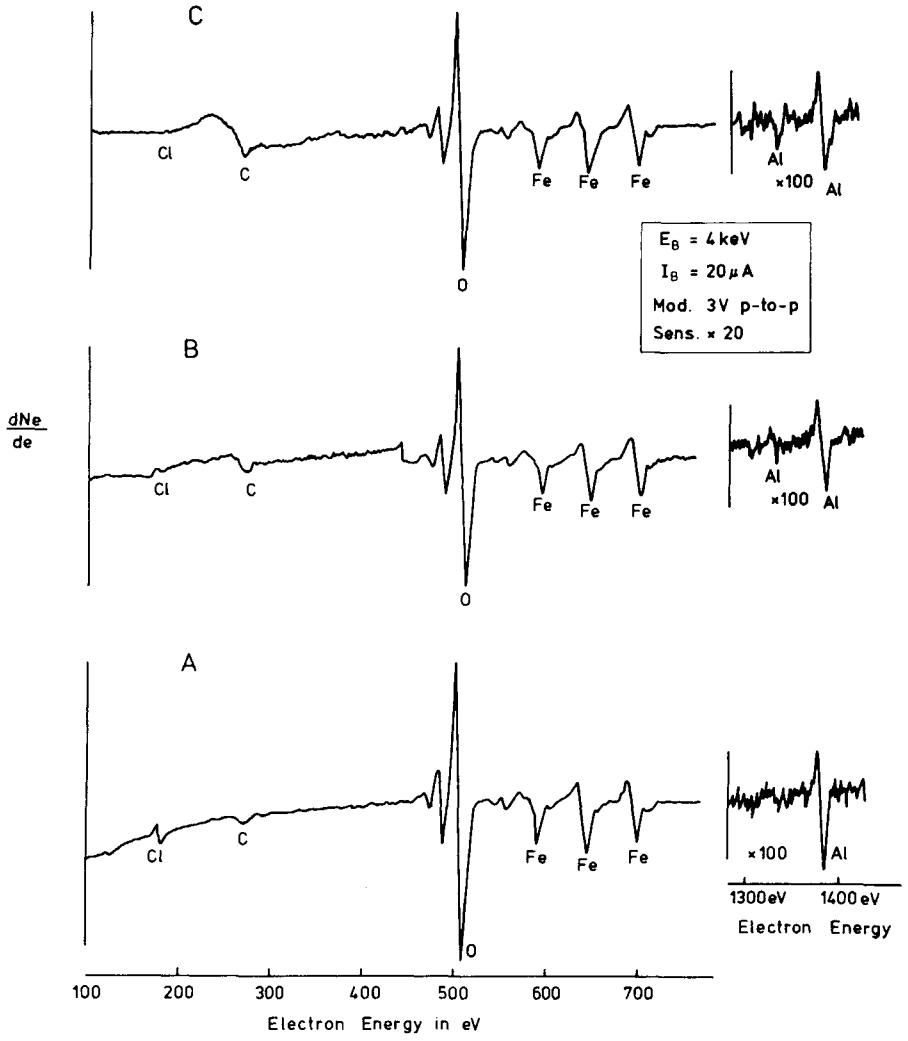

Fig. 5. AES spectra taken from points A, B, and C. Note small carbon peak at 271 eV.

where fracture occurred with epoxy covering the stainless steel. Photoelectron peaks characteristic of components of the stainless steel were detected, suggesting that epoxide coverage of the surface was not complete.

Not surprisingly, the concentration of carbon on the epoxide surface was high with the element existing in two chemical states (288.0, 289.5 eV) prior to ion bombardment. This doublet was found whenever freshly fractured epoxide was analyzed and thus can almost certainly be said to be characteristic of epoxy resin. The carbon species of *BE* 286.4 eV which was found after removal of 50 Å of material (and also found on metal surfaces) may be due to a polymer in intimate contact with the metal oxide surface since Wyatt et al.[23] observed a similar binding energy for C(1*s*) for a polyurethane adhesive in contact with an aluminum surface. After erosion of the surface to a depth of 130 Å, only one carbon peak (*BE* ~284.5 eV, typical of a hydrocarbon or elemental carbon) was detected. It should be emphasized that prolonged ion bombardment leads to a degradation of most organic species to carbon, resulting in a loss of chemical information.

No satisfactory explanation can be put forward for the observed concentrations of nitrogen and chlorine, except that the latter may be due to traces of trichloroethylene used in the cleaning process. Information from AES was not possible from the epoxide surfaces, as charging of the surface by the primary electron beam produced excessive spectral distortion.

Water-Soaked Unprimed Joints

On fracture, the water-soaked joints released a considerable amount of gas which raised the system pressure momentarily from 8×10^{-10} torr to 3×10^{-7} torr. Almost all the gas evolved was water vapor. All the samples broke by apparently interfacial failure, with the crack path jumping from one interface to the other and hence leaving clumps of adhesive on both fractured surfaces; a typical SEM photograph of one of the surfaces is shown in Figure 4. Auger analyses were carried out on the "metal" surface at points A, B, and C (Fig. 4), and the spectra recorded are presented in Figure 5. It is clear from these spectra that the carbon concentration over the metal fraction of the surface was low ($\leq$ 5%), suggesting that little organic material existed on the "metal" surface.

From these AES results it can be concluded that virtually all the carbon de-

TABLE VII
Water-Soaked Unprimed Joints. Variation in Surface Concentration of Elements Detected by XPS[a]

Element	Surface concn., atomic %, freshly fractured surface	Surface concn. after indicated amount of material removed		
		50 Å	130 Å	640 Å
Fe	10.5	10.5	33.7	27.1
O	65.0	55.5	50.2	59.9
C	21.0	7.8	12.6	8.3
N	—	—	—	—
Cl	—	—	2.5	0.8
Al	—	3.0	4.8	3.9
F	3.5	—	—	—

[a] Estimated error ± 15%.

TABLE VIII
Water-Soaked Unprimed Joints. Variation of Binding Energy of Iron, Oxygen, and Carbon[a]

Element	Binding energy, eV, freshly fractured surface	Binding energy after indicated amount of material removed		
		50 Å	130 Å	640 Å
Fe	715.0 710.2 (d)	710	710	709.8 706.2 (Sh)
O	536.2 531.2 (d)	530	529.9	529.9
C	288.2 290.1 (Sh)	287.5 284.7 (d)	287.5 284.8 (d)	284.9

[a] Sh = Shoulder on main peak; d = doublet. Error ±0.4 eV.

tected by XPS, ~21% (see Table VII), was associated with the epoxide, which covered some 10% of the analyzed surface. This conclusion is reinforced by the detection of the carbon doublet (see Table VIII) ascribed in the previous section to the epoxy resin. After prolonged ion bombardment, the carbonaceous material was reduced either to elemental carbon or to a hydrocarbon.

In the XPS analyses, an iron peak was found at a binding energy of 715.0 eV, that is, some 2 eV higher than that observed from either the dry or the silane-primed specimens. Since so much water was evolved on fracture and since it must have been present originally at the interface, it is tentatively suggested that the iron species of *BE* 715.0 eV, together with the oxygen of *be* 536.2 eV, derived from a heavily hydrated iron oxide onto which a considerable amount of water had been chemisorbed. Light ion bombardment to a depth of 50 Å removed both iron and oxygen peaks associated with the hydrated iron. The iron peak at 710.2 eV and the oxygen peak at 531.2 eV can be ascribed to a more stable iron oxide. Since pure iron (*BE* 706.5 eV) appeared only weakly at a depth of 640 Å, the oxide layer on the "metal" surface must have been over 600 Å thick, a considerably thicker layer than observed on the dry specimens.

TABLE IX
Water-Soaked Primed Joint. "Metal" Surface: Variation in Surface Concentration of Elements Detected by XPS[a]

Element	Surface concn., atomic %, freshly fractured surface	Surface concn. after indicated amount of material removed		
		50 Å	130 Å	400 Å
Fe	21.5	39.5	50.9	67.2
O	60.9	45.9	38.6	27.6
C	7.4	2.5	1.8	1.8
N	—	—	—	—
Cl	3.0	1.7	0.9	—
Al	5.8	8.4	7.8	3.4
Si	1.4	2.0	—	—
F	—	—	—	—

[a] Estimated error ± 15%.

TABLE X
Water-Soaked Primed Joint. "Metal" Surface: Variation of Binding Energy of Iron, Carbon, and Oxygen[a]

Element	Binding energy, eV, freshly fractured surface	Binding energy after indicated amount of material removed		
		50 Å	130 Å	400 Å
Fe	709.5	708.7	708.5	705.8
		705.7 (Sh)	705.2 (Sh)	708.5 (Sh)
O	531.2	530.2	530.2	530.5
	529.2 (Sh)			
C	286.8	284.2	284.2	unassignable
		286.2 (Sh)		

[a] Sh = Shoulder on main peak. Error ± 0.4 eV.

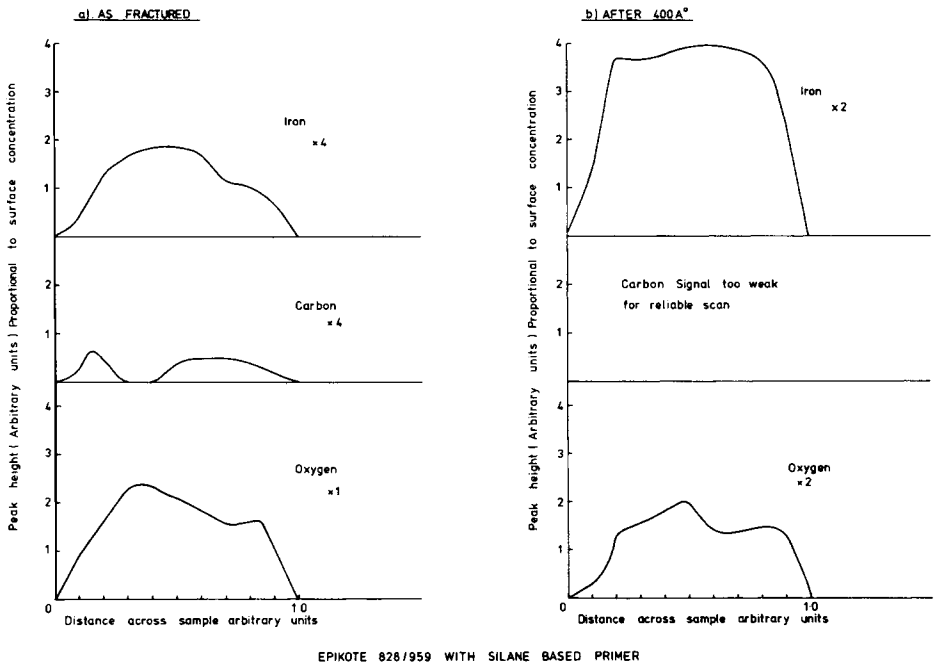

Fig. 6. AES "line scans" taken from the "metal" side of a water-soaked primed joint. Note the patchiness of the carbon over the surface and the increase of both iron and oxygen after removal of 400 Å.

Water-Soaked Primed Joints

When fractured, the silane-primed joints produced a momentary pressure rise comparable in magnitude to that observed for the dry joints. The five specimens broke such that two "metal" and three "epoxide" surfaces could be presented for analysis.

The XPS analyses of the as-fractured metal surfaces revealed (see Tables IX and X) that the iron existed in the dry iron oxide form while the carbon existed in a form ascribable to a polymer existing in contact with a metal. Erosion of surface revealed increased amounts of iron whose chemical state changed from the oxide (20%) to an almost pure metal state (80%) at a depth of 400 Å. Coupled to this increasing Fe concentration with depth was a decreasing carbon concentration. All the excess oxygen found at this depth could be ascribed to oxygen in the alumina and in traces of iron oxide.

It was found possible to perform AES on the metal surfaces, and "line scans" similar to those performed for the dry joints were taken for carbon, oxygen, and iron. Results are presented in Figure 6. Areas of high carbon concentration corresponded to areas of low iron and oxygen concentrations, suggesting a patchwork arrangement of carbonaceous polymer material existing over the metal surface. Removal of 400 Å of surface resulted in a removal of this carbonaceous material and an increase in the iron concentration, which at this depth was found (by XPS) to be almost entirely pure metal.

The XPS analyses of the epoxide surfaces (see Tables XI and XII) revealed that the carbon existed in the two forms ascribed earlier to the epoxy resin (i.e., with binding energies 288.0 eV and 289.7 eV) and that removal of the surface layer

resulted in more carbon being exposed. The iron and oxygen existing on the as-fractured surface can be ascribed to hydrated iron oxide which, on ion bombardment, reduced to the normal oxide existing on the surface by dry iron. Some 12% iron was detected at a depth of 400 Å, an estimated 10% of which existed as pure metal. The presence of the iron at this depth can be explained by the previously mentioned pinhole theory.

Since 12% of the atoms in the primer were silicon, then, provided the metal surface is covered by a film of the primer greater than 10 Å thick, this concentration of the silicon should be detected. It was found, however, that the amount of silicon residing on the "epoxide" and "metal" surfaces was about the same, the total concentration being about 4.0%. To clarify this anomaly, a cleaned mild steel specimen was coated with a similar amount of primer as used for the primed joints and analyzed using XPS; no silicon was detected, suggesting that the solution volatilized on being subjected to vacuum. This volatilization was thought to be due either to a lack of polymerization or to failure of the silane to chemisorb. Addition of a 1% solution of the amine HY 959 to the primer catalyzed polymerization of the silane, following which XPS analysis (see Table XIII) revealed that 5% silicon existed at the surface. The latter value is in close agreement with

TABLE XI
• Water-Soaked Primed Joint. Epoxide Surface: Variation in Surface Concentration of Elements Detected by XPS[a]

Element	Surface concn., atomic %, freshly fractured surface	Surface concn. after indicated amount of material removed		
		50 Å	130 Å	400 Å
Fe	5.0	9.3	9.9	11.8
O	48.9	40.1	36.2	31.1
C	34.3	43.3	45.6	51.1
N	2.4	—	—	—
Cl	3.7	2.7	3.5	2.0
Al	0.9	1.8	2.4	2.0
Si	1.8	2.8	2.4	2.0
F	3.0	—	—	—

[a] Estimated error ± 15%.

TABLE XII
Water-Soaked Primed Joint. Epoxide Surface: Variation of Binding Energy of Iron, Carbon, and Oxygen[a]

Element	Binding energy, eV, freshly fractured surface	Binding energy after indicated amount of material removed		
		50 Å	130 Å	400 Å
Fe	713.7	712.5	711.7 710.2 (Sh)	709.2 706.2 (Sh)
O	536.2	533.7	532.5 535.5 (Sh)	531.2
C	288.0 289.7 (Sh)	287.7	286.0	284.2

[a] Sh = Shoulder on main peak. Error ± 0.4 eV.

the total silicon concentration detected on the two fracture surfaces (4.5%), suggesting that the silane primer does not cover the fracture surface completely after polymerization.

DISCUSSION

Dry Joints

From the XPS results it is clear that, after fracturing the joint, not only was an appreciable amount of carbon left on the "metal" surface but also that it existed in a different chemical environment from that found on the mild steel reference sample. The observed shift in binding energy to 286.4 eV has been attributed here to a polymer in intimate contact with the surface. The question of how this polymer is distributed across the sample now arises.

The fact that strong iron and oxygen signals were obtained in both XPS and AES rules out the possibility that the polymer existed as a continuous film greater than about 20 Å thick, since the mean free path of a 1000-eV electron is estimated from other work[24,25] to be of that order. Further, as metallic iron was present after ion bombardment, the polymer cannot have covered the surface completely. The Auger line profiles (Fig. 2), however, indicate that the concentrations of carbon, oxygen, and iron were evenly distributed across the sample. Since the diameter of the electron beam was 30 μm, these results would suggest that neither the iron, iron oxide, nor polymer existed in areas greater in diameter than that of the electron probe.

It is postulated that the fracture propagated very close to the epoxide/metal interface; a diagram illustrating the proposed path of failure is given in Figure 7. Some epoxide was left buried in crevices in the metal surface, and in places the fracture actually passed through the metal substrate itself. It would seem that any corrosion products came away with the epoxide surface. A consideration of the results obtained from the epoxide surface shows that holes were probably present in the adhesive and also that a certain amount of corrosion of the metal substrate had occurred.

Water-Soaked Unprimed Joints

These joints broke by interfacial failure between the oxide and adhesive, but the crack jumped from one interface to the other during fracture leaving part of the surface covered in epoxy resin and part apparently free of epoxy. The Auger analysis of the "metal" at points A, B, and C (Fig. 4) showed that very little carbon was present on that part of the surface, ssggesting a clean break between the epoxide and the metal substrate. Analysis by XPS showed that the doublet

TABLE XIII
Silane Control Experiment. Surface Concentration of Elements Detected by XPS

Element	Surface concn., atomic %
Fe	11.1%
O	45.1%
C	38.6%
Si	5.2%

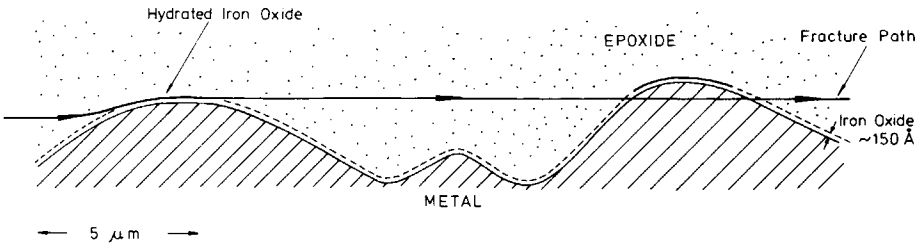

Fig. 7. Proposed model for the fracture path of a dry, unprimed epoxy resin joint. Epoxy resin exists in the deep valleys while small areas of pure metal and hydrated iron oxide are exposed.

typical of the bulk epoxide was detected (presumably coming from the visible lump of adhesive which was estimated to cover some 10% of the analyzed area), and this precludes the possibility of the crack path being solely through the oxide layer.

The XPS results also indicated that the iron oxide thickness had increased from the 100 Å observed on mild steel to at least 640 Å and that some of the iron existed in a heavily hydrated state. Using somewhat cruder analytical techniques, Kinloch and Gledhill[6] have proposed that for joints similar to those investigated here, water should initially displace the adhesive from the metal surface and that corrosion would follow subsequently. The results presented here are in general agreement with their findings, since water was certainly present at the interface and corrosion definitely had occurred. It is impossible to say, however, from the present experiments whether displacement of the adhesive by water alone caused joint failure or whether failure occurred owing to simultaneous adhesive displacement and corrosion.

Water-Soaked Primed Joints

Silicon from the silane primer was found on each of the fractured surfaces from the above joints, with the concentration on each being approximately 2.5 atomic percent. The control experiment in which a similar amount of silane solution was polymerized on a mild steel surface gave a silicon concentration of 5%, a value very close to the total amount detected on the two surfaces, thus suggesting that the fracture had proceeded within the silane layer. The Auger line profile of the "metal" surface indicated that the specimen was covered by a patchy layer of some carbonaceous material; and as a C(1*s*) peak at 286.8 eV was observed, the layer can be attributed to the polymerized silane. The presence of some hydrated iron oxide brought about by water corrosion of the substrate supports further the contention that the silane covering was incomplete. Nevertheless, the primer did offer a considerable amount of protection to the metal since here, the iron oxide thickness was only marginally greater than that found on the mild steel sample.

Therefore, although previous work[7,26] has demonstrated that the presence of a silane primer may increase the environmental stability of adhesive joints, the above results suggest that the silane primer is now the weakest link in the joint and fracture occurs by cohesive failure of this layer. This conclusion is in agreement with results reported from radioisotope studies[27] on debonded glass–γ-aminopropyltriethoxysilane primer–epoxy adhesive joints and in both

cases may possibly arise from hydrolysis of siloxane bonds in the silane primer structure, which, as discussed previously, is essentially a polysiloxane network. The present spectroscopic studies have not revealed whether the silane primer is physisorbed or chemisorbed onto the metal oxide surface.

CONCLUSIONS

Although prior to water immersion, the unprimed mild steel–epoxy joints appeared visually to fail at the metal oxide–epoxy interface, AES and XPS analysis has clearly demonstrated that the actual failure pattern is far more complex. The crack propagated close to, but not exactly at, the interface, traveling partially through the adhesive (leaving epoxide material buried in crevices in the metal substrate surface) and in places even through the metal substrate itself. Whether this failure pattern arises from a weak boundary layer of adhesive close to the interface or stress concentration effects[28,29] has yet to be resolved.

After exposure to water, the fracture path is exactly between the adhesive–metal oxide interface, and corrosion of the iron oxide leads to a considerable increase in the oxide thickness. When a silane-based primer is employed which is known to increase joint durability, the polysiloxane–metal oxide interface appears to be resistant to water attack, and the primer itself is now the weakest part of the joint, fracture occurring by cohesive failure of this layer.

Thus, AES and XPS have proved to be invaluable analytical techniques for identifying exactly the locus of joint failure and it appears that to increase joint durability further, attention should be focused on increasing the intrinsic strength of the silane-based primers commonly employed.

The paper is published by permission of the Controller, Her Majesty's Stationery Office, holder of Crown Copyright, London 1976. The authors would like to thank Dr. John Riviere and Dr. Paul Coad for their helpful discussions during the course of this study.

References

1. W. C. Wake, in *Aspects of Adhesion*, Vol. 7, D. J. Alner, Ed., University Press, London, 1969, p. 64.
2. R. F. Wegman, *Appl. Polym. Symp.*, **19**, 385 (1972).
3. J. J. Bikerman, *The Science of Adhesive Joints*, 2nd ed., Academic Press, New York, (1968).
4. C. Kerr, N. C. Macdonald, and S. Orman, *J. Appl. Chem.*, **17**, 62 (1967).
5. G. S. Koboyashi and D. J. Donnelly, Boeing Aircraft Company Report D6-41517, 1974.
6. R. Gledhill and A. J. Kinloch, *J. Adhesion*, **6**, 315 (1974).
7. A. J. Kinloch, W. A. DuKes, and R. A. Gledhill, *Amer. Chem. Soc. Prepr.*, **35**(1), 546 (1975).
8. W. A. Zisman, *Ind. Eng. Chem., Prod. Res. Dev*, **8**(2), 99 (1969).
9. W. D. Bascom and R. L. Patrick, *Adhesive Age*, **17**, 25 (1974).
10. W. D. Bascom, *Macromolecules*, **5**, 792 (1972).
11. C. R. Brundle, *Appl. Spectrosc.*, **25**, 8 (1971).
12. C. C. Chang, *Surf. Sci.*, **25**, 53 (1974).
13. N. C. Macdonald and J. R. Waldrop, *Appl. Phys. Lett.*, **19**(9), 315 (1971).
14. P. W. Palmberg, *J. Elect. Spectrosc.*, **5**, 691 (1974).
15. M. Gettings and J. P. Coad, *Surf. Sci.*, **53**, 636 (1975).
16. K. Hirokawa, F. Honda, and M. Oku, *J. Elect. Spectrosc.*, **6**, 333 (1975).
17. D. Briggs, *Disc. Faraday Soc.* (1975).

18. M. K. Bahl, *J. Phys., F.: Metal Phys.*, **4,** 497 (1974).
19. J. C. Fuggle, L. M. Watson, D. J. Fabian, and S. Affrossman, *Surf. Sci.*, **49,** 61 (1975).
20. J. P. Coad, private communication.
21. F. R. McFeeley, S. P. Kowalczyk, L. Ley, R. G. Cavell, R. A. Pollak, and D. A. Shirley, *Phys. Rev. B* **9,** 5268 (1974).
22. U. Gelius, P. F. Heden, J. Hedman, B. J. Lindberg, R. Manne, R. Nordberg, C. Nording, and K. Siegbahn, *Phys. Scripta,* **2,** 70 (1970).
23. D. M. Wyatt, R. C. Grey, J. C. Carver, D. M. Hercules, and L. Masters, *Appl. Spectrosc.*, **28,** 439 (1974).
24. C . R. Brundle, *Surf. Sci.*, **48,** 99 (1975).
25. C. J. Powell, *Surf. Sci.*, **44,** 29 (1974).
26. R. L. Patrick, J. A. Brown, and L. Dunbar, U.S. Naval Air System Command Final Report No. 0019-70-C-0184, (1970).
27. M. E. Schroder, *J. Adhesion,* **2,** 202 (1970).
28. C. W. Jennings, *J. Adhesion,* **4,** 25 (1972).
29. W. D. Bascom, C. O. Timmons, and R. L. Jones, *J. Mat. Sci.*, **10,** 1037 (1975).

Received April 16, 1976
Revised July 15, 1976